An Information Potential Approach for Tracking and Surveilling Multiple Moving Targets using Mobile Sensor Agents

W. Lu[§], G. Zhang[§], S. Ferrari[§], R. Fierro[†], and I. Palunko[†]

[§]Laboratory for Intelligent Systems and Control (LISC), Department of Mechanical Engineering and Materials Science, Duke University, Durham, NC, USA;
[†]Multi-Agent, Robotics, Hybrid, and Embedded Systems Laboratory Department of Electrical and Computer Engineering University of New Mexico, Albuquerque, NM, USA.

ABSTRACT

The problem of surveilling moving targets using mobile sensor agents (MSAs) is applicable to a variety of fields, including environmental monitoring, security, and manufacturing. Several authors have shown that the performance of a mobile sensor can be greatly improved by planning its motion and control strategies based on its sensing objectives. This paper presents an information potential approach for computing the MSAs' motion plans and control inputs based on the feedback from a modified particle filter used for tracking moving targets. The modified particle filter, as presented in this paper implements a new sampling method (based on supporting intervals of density functions), which accounts for the latest sensor measurements and adapts, accordingly, a mixture representation of the probability density functions (PDFs) for the target motion. It is assumed that the target motion can be modeled as a semi-Markov jump process, and that the PDFs of the Markov parameters can be updated based on real-time sensor measurements by a centralized processing unit or MSAs supervisor. Subsequently, the MSAs supervisor computes an information potential function that is communicated to the sensors, and used to determine their individual feedback control inputs, such that sensors with bounded field-of-view (FOV) can follow and surveil the target over time.

Keywords: Target tracking, surveillance, mobile sensor networks, multi-agent systems, information value, potential field, particle filtering.

1. INTRODUCTION

The paradigm of the moving target surveillance using a network of mobile sensor agents (MSAs) is found in a variety of applications, including the monitoring of urban environments,[1] tracking anomalies in merchandise, manufacturing plants,[2] or information, and tracking of endangered species in a wild area.[3] Modern surveillance systems often consist of MSAs deployed to detect and track moving targets in a complex and unstructured environment. A mobile sensor agent, comprised of an autonomous vehicle equipped with embedded wireless sensors and communication devices, is often deployed to cooperatively track and surveil moving targets based on limited information that only becomes available when the target enters a sensor's field-of-view (FOV) or visibility region. Typically, the objectives are to maximize tracking accuracy and reliability by means of limited sensor resources, namely energy and communications. Thus, the MSAs' performance can be greatly improved by planning the sensor's motion and control, and by taking into account the FOV geometry, the sensor dynamics, and the target measurements that become available over time.[1,4–8] In particular, when the sensor's FOV is bounded, the sensor's position and orientation determine what targets can be measured at any given time. Therefore, the sensor path must be planned in concert with the measurement sequence.

Cell decomposition[4,9] and probabilistic roadmap methods[8] have been successfully developed for solving geometric sensor path planning problems with stationary targets, such as the treasure hunt. Visibility-based methods

Further author information: (Send correspondence to W.L.)
W.L., G.Z., and S.F.: E-mail: {wenjie.lu, guoxian.zhang, sferrari}@duke.edu, Telephone: 1 919 660 5305
R.F., and I.P.: E-mail: {rfierro, ipalunko}@ece.unm.edu, Telephone: 1 505 277 4125

Unmanned Systems Technology XIII, edited by Douglas W. Gage, Charles M. Shoemaker, Robert E. Karlsen, Grant R. Gerhart, Proc. of SPIE Vol. 8045, 80450T · © 2011 SPIE
CCC code: 0277-786X/11/$18 · doi: 10.1117/12.884116

have been proposed in.[10–13] to account for the sensor's dynamics and FOV. However, existing methods typically are not applicable to moving targets, and do not account for the uncertainty associated with target tracking, for example the uncertainty due to complex environmental conditions and online sensor measurements, where, tracking refers to the estimation of the state of a moving target through one or more sensors. The problems of data association and fusion that arise in tracking multiple targets by means of multiple sensors have received considerable attention.[14–18] Typically, in these problems the target is modeled as a linear dynamic system with random disturbance inputs, and its state is predicted through frequent observations of its measurable output, which include additive random noise characterized by a Gaussian distribution. Kalman filter equations are then used to optimally estimate the target state based on the sensor measurements collected over time. While this approach is well suited to long-range high-accuracy sensors, such as radars, and their applications, many of the underlying assumptions are violated in MSAs, because the targets are non-cooperative and inherently random, and the sensor measurement errors are not additive and non-Gaussian. Furthermore, there is no systematic approach for incorporating the results of the tracking algorithms and the effects of environmental and operating conditions into the motion planning problem.

In this paper, a novel potential function method is developed for planning the sensor path and control inputs based on the feedback provided by the target tracking algorithm. While the classical Kalman filter[19] assumes that the target dynamic and output equations are linear, and the random inputs can be modeled by a Gaussian distribution, the extended Kalman filter (EKF)[20] can be used when the system dynamics can be linearized about nominal values predicted by a Taylor expansion. The unscented Kalman filter (UKF)[21] is based on the knowledge of the mean and the covariance of a given function by the unscented transformation (UT) method,[22] and can be applied to compute the mean and covariance of a function up to the second order of the Taylor expansion. However, the efficiency of these filters tends to decrease as the system dynamics become highly nonlinear, as due to increasingly stringent and complex operating and environmental conditions. Thus, a non-parametric method based on condensation and Monte Carlo simulation, known as particle filter, has been proposed[23] for tracking multiple targets exhibiting nonlinear dynamics and non-Gaussian random effects.

Particle filters are well suited to modern surveillance applications because they can be used to estimate Bayesian models in which the hidden variables are connected by a Markov chain, over discrete time, but the targets' state is continuous, as in Markov motion models. In the particle filter method, a weighted set of particles or point masses are used to represent the PDF of the target state by means of a superposition of weighted Dirac delta functions.[24] At each iteration of the particle filter, particles representing possible target state are sampled from an importance density function.[25] The weight associated with each particle is obtained from the target-state likelihood function and the prior estimation PDF of the target state. When the effective particle size is smaller than a predefined threshold, a re-sampling technique is implemented, as explained in.[26] One disadvantage of conventional particle-filtering techniques is that the target-state transition function is used as the importance density function to sample particles, without taking new observations into account.[27] As a result, when the target state transition function is much broader than the likelihood function, few sampled particles have proper locations and weights. An improved particle filter, the unscented particle filter (UPF) was proposed in,[27] to overcome this difficulty, by combining UKF and the particle-filtering technique. The UKF generates a proposed distribution in which the current measurements are considered, and then the distribution is used as the importance density to sample particles.

Another disadvantage of particle filters is that the point-mass representation provides limited information about the estimated PDF of the target state, and does not account for the targets' dynamic equations. To overcome both of these disadvantages of existing particle-filter tracking algorithms, this paper presents a new sampling method and a new representation for the approximation of the target state PDF that also accounts for the target dynamics. In the proposed method, the target dynamics are modeled by a semi-Markov jump process, and the particles are sampled based on the supporting intervals of the target-state likelihood function and the prior estimation function of the target state. Where, the supporting interval of a distribution is defined as the 90% confidence interval.[28] The weight for each particle is obtained by considering the likelihood function and the transition function simultaneously. Then, the weighted expectation maximization (EM) algorithm is implemented to use the sampled weighted particles to generate a normal mixture model of the distribution. Unlike the Dirac-delta representation, the normal mixture model of the target-state PDF can then be easily combined with the target-dynamic equation. A potential field method is developed to plan the sensor motion and control such that each sensor can surveil a target, by maintaining a predefined distance between its platform and the target, such that the target remains inside the sensor's FOV. The stability of the resulting sensor control law is guaranteed using Lyapunov stability theory.

This paper is organized as follows. Section 2 describes the tracking and surveillance problem formulation and assumptions. The background on the particle filter and the potential field methods is reviewed in Section 3. Section 4 describes the new sampling method used in particle filter and the mixture Gaussian distribution representation for the approximation of the target state PDF, as well as a modified potential field method. The simulations and results are shown in Section 5. Conclusions and future work are given in Section 6.

2. PROBLEM FORMULATION AND ASSUMPTIONS

The problem considered in this paper consists of determining the motion and control law of a MSA, indexed by $i \in I_S$, deployed for the purpose of tracking and surveilling a moving point-mass target, indexed by $j \in I_T\mathcal{T}$, in a region of interest (ROI) comprised of a bounded, two-dimensional Euclidian workspace $\mathcal{W} \in \mathbb{R}^2$. Where, I_S and I_T denote the index sets of the network of MSAs and targets, respectively, and it is assumed that the assignment problem has been resolved through multitarget-multisensor data association and assignment algorithms.[29,30] The sensor has platform geometry $\mathcal{A}_i \in \mathbb{R}^2$, and a bounded FOV $\mathcal{S}_i \in \mathbb{R}^2$. $\mathcal{F}_{\mathcal{A}_i}$ is a moving Cartesian frame embedded in $\mathcal{A}_i$ such that every point of $\mathcal{A}_i$, and every point of $\mathcal{S}_i$, have fixed positions with respect to $\mathcal{F}_{\mathcal{A}_i}$. Then, using a suitable transformation, the ith sensor state $\mathbf{Y}_i^\kappa = [x_i^\kappa \; y_i^\kappa \; \dot{x}_i^\kappa \; \dot{y}_i^\kappa]^T$ can be used to specify the position and orientation of all points in $\mathcal{A}_i$ and $\mathcal{S}_j$ at t_κ, with respect to a fixed inertial frame $\mathcal{F}_{\mathcal{W}}$, embedded in $\mathcal{W}$. Where, x_i^κ and y_i^κ are the coordinates of the ith sensor in $\mathcal{F}_{\mathcal{W}}$, and $\dot{x}_i^\kappa$ and $\dot{y}_i^\kappa$ are its linear velocities in $\mathcal{F}_{\mathcal{W}}$. Additionally, let $\mathbf{v}_i^\kappa = [x_i^\kappa, y_i^\kappa]^T$. Now, let ρ_{ij} denote the geometric distance between the origin of $\mathcal{F}_{\mathcal{A}_i}$ and its nearest target j in $\mathcal{W}$. Then, the objective of the ith MSA is to maintain ρ_{ij} within a predefined range,

$$\rho_0 < \rho_{ij} < \rho_1 \tag{1}$$

while avoiding a set of known, fixed, and rigid obstacles in $\mathcal{W}$, denoted by $\mathcal{B}_l$, $l \in I_B$. Where, I_B is an obstacle index set, and ρ_0 and ρ_1 are constant parameters specified by the user.

In this paper, it is assumed that the FOV of every sensor $i \in I_S$ is a disk $\mathcal{S}_i \in \mathbb{R}^2$ with radius r. The sensor dynamics are assumed to be linear and time-invariant (LTI), and to be discretized with respect to time, such that the sensor state transition function can be written in state-space form as,

$$\mathbf{Y}_i^{\kappa+1} = \mathbf{A}\mathbf{Y}_i^\kappa + \begin{bmatrix} 0 \\ 0 \\ \delta \end{bmatrix} \mathbf{u}_i^\kappa, \quad \text{for} \quad \kappa = 0, 1, \ldots, \tag{2}$$

where, κ is the time index, δ is the time span between $t^{\kappa+1}$ and t^κ, $\mathbf{u}_i \in \mathbb{R}^2$ is the control vector, $\dot{\mathbf{v}}_i^\kappa = \mathbf{u}_i^\kappa$, and,

$$\mathbf{A} \equiv \begin{bmatrix} 1 & 0 & \delta & 0 \\ 0 & 1 & 0 & \delta \\ 0 & 0 & 1 & 0 \\ 0 & 0 & 0 & 1 \end{bmatrix} \tag{3}$$

For simplicity, the sensor geometry is assumed to only translate in $\mathcal{W}$, such that the heading of the sensor is maintained constant at all times.

The motion of target $j \in I_T$ is modeled as a continuous-time Markov motion process, also known as semi-Markov jump process,[31] where, we say that x_t is a *continuous-time Markov process* if for $0 \leq t_0 < \cdots < t_{k-1} < t_k < t$ we have $\Pr(x_t \in B \mid x_k = s_k, x_{k-1} = s_{k-1}, \cdots, x_0 = s_0) = \Pr(x_t \in B \mid x_k = s_k)$ where Pr denotes the probability transition function, and $s_1, \ldots, s_k \in \mathcal{X}$ are realizations of the state space $\mathcal{X}$. Now, let the random variables θ_j^k and v_j^k represent the jth target's heading and velocity, respectively, during the time interval $\Delta t_k = (t_{k+1} - t_k)$, $k = 1, 2, \ldots$. Then, the target motion can be modeled as a continuous-time Markov process with a family of random variables $\{\mathbf{x}_j^k, \theta_j^k, v_j^k\}$, where $\mathbf{x}_j^k \in \mathcal{W}$ is the jth target position at t_k. A three-dimensional real-valued vector function maps the family of random variables $\{\theta_j^k, v_j^k\}$ into the random vector

$\mathbf{x}_j(t)$, representing the target position at every time $t \in [t_0,\ t_f]$, such that the value of the target motion process is given by,

$$\dot{\mathbf{x}}_j(t) = v_j(t)[\cos\theta_j(t) \quad \sin\theta_j(t)]^T, \tag{4}$$

and, therefore, the motion of target j is a Markov process. The third component of the vector function is the identity function. It follows that θ_j and v_j are piece-wise constant, while $\mathbf{x}_j$ has discontinuities at the time instants t_k, when the target j changes its heading and velocity. In this paper, it is assumed that the instants when the target changes its heading are known *a-priori*, and all targets move at a constant speed $v_j = v$. Also, it assumed that all time intervals are of constant length, i.e., $\Delta t_k = \tau$, for $\forall k$.

Now, let $\mathbf{X}_j^k = [\mathbf{x}_j^k\ \theta_j^k]^T$ denote the jth target state at time step k. The probability transition function for the target heading at the instant t_k of a discontinuity, is defined as,

$$f(\theta_j^{k+1} \mid \theta_j^k) = \mathcal{N}(\theta_j^{k+1} \mid \mu + \theta_j^k, \sigma^2) \tag{5}$$

where the mean of heading change μ and the variance of the heading change σ are constant parameters that are assumed known *a-priori*. The target heading remains constant during every time interval Δt_k, The target state transition function at every discontinuity is given by,

$$\mathbf{X}_i^{k+1} \quad = \quad \mathbf{X}_j^k + \begin{bmatrix} \cos(\theta_j^k)\tau v \\ \sin(\theta_j^k)\tau v \\ \mathcal{N}(\mu, \sigma^2) \end{bmatrix}, \quad \text{for} \quad \forall k. \tag{6}$$

where τ is the known length of the time interval Δt_k.

The MSA network attempts to obtain measurements of the targets' positions once with a frequency of $1/\delta$ (Hz), where $\delta < \tau$. Thus, if a time instant t_κ, the jth target is inside the ith sensor's FOV, then the ith MSA can obtain a measurement of the jth target position,

$$\mathbf{z}_i^\kappa = \mathbf{x}_j^\kappa + \nu_{ij} \iff \mathbf{x}_j(t_\kappa) \in \mathcal{S}_i \tag{7}$$

where $\mathbf{x}_j^\kappa$ is the jth target's position at time t_κ, and ν_{ij} is a white-noise error with standard deviation Σ_{ij}. If $\mathbf{x}_j(t_\kappa) \notin \mathcal{S}_i$, no measurements are returned to the ith sensor.

3. BACKGROUND

3.1 Particle Filter Methods

The particle filter technique is a recursive model estimation technique based on sequential Monte Carlo. It is applicable to nonlinear system dynamics, with non-Gaussian random inputs. Moreover, because of their recursive nature, particle filters are easily applicable to online data processing and estimation. The main idea of particle filters is to represent the PDF functions with properly weighted and relocated point-mass, known as particles. These particles are sampled from an importance density which is crucial to the particle filter algorithm. Let $\{\mathbf{x}_{j,p}^\kappa, w_{j,p}^\kappa\}_{p=1}^N$ denote the weighted particles that are used to approximate the posterior PDF $f(\mathbf{x}_j^\kappa \mid Z_j^\kappa)$ for the jth target at t_κ, where $Z_j^\kappa = \{\mathbf{z}_j^0, \ldots, \mathbf{z}_j^\kappa\}$ denotes the set of all measurements obtained by sensor i, from target j, up to t_κ. Then, the posterior probability density function of the target state, given the measurement at t_κ can be modeled as,

$$f(\mathbf{x}_j^\kappa \mid Z_j^\kappa) = \sum_{p=1}^N w_{j,p}^\kappa \delta(\mathbf{x}_{j,p}^\kappa), \quad \sum_{p=1}^N w_{j,p}^\kappa = 1 \tag{8}$$

where $w_{j,p}^\kappa$ is non-negative and δ is the Dirac delta function.[23] Although different particle filter techniques have been proposed,[25] the techniques always consist of the recursive propagation of the particles and the particle weights. In each iteration, the particles $\mathbf{x}_{j,p}^\kappa$ are sampled from the importance density $q(\mathbf{x})$. Then, weight $w_{j,p}^k$ is updated for each particle by

$$w_{j,p}^\kappa \propto \frac{p(\mathbf{x}_{j,p}^\kappa)}{q(\mathbf{x}_{j,p}^\kappa)} \tag{9}$$

where $p(\mathbf{x}^{\kappa}_{j,p}) \propto f(\mathbf{x}^{\kappa}_{j,p} \mid Z^{\kappa}_{j})$. Additionally, the weights are normalized at the end of each iteration.

The target state transition function is used as the importance density function. Thus, the sampled particles can not fully represent the target state estimation since they are sampled without considering the new measurement. Another common drawback of particle filters is the degeneracy phenomenon,[27] i.e., the variance of particle weights accumulates along iterations. This phenomenon indicates that a number of particles have low weights and no contributions in approximating the probability density function $f(\mathbf{x}^{\kappa}_{j} \mid \mathbf{z}^{\kappa}_{j})$ but put heavy computational burden to the algorithm. A common way to evaluate the degeneracy phenomenon is the effective sample size N_e,[26] obtained by

$$N_e = \frac{1}{\sum_{p=1}^{N}(w^{\kappa}_{j,p})^2} \tag{10}$$

where $w^{\kappa}_{j,p},\ p = 1, 2, \ldots, N$ are the normalized weights. In general, a re-sampling procedure is taken when $N_e < N_s$, where N_s is a predefined threshold, and is usually set as $\frac{N}{2}$. Let $\{\mathbf{x}^{\kappa}_{j,p}, w^{\kappa}_{j,p}\}^{N}_{p=1}$ denote the particle set that needs to be re-sampled, and let $\{\mathbf{x}^{\kappa*}_{j,p}, w^{\kappa*}_{j,p}\}^{N}_{p=1}$ denote the particle set after re-sampling. The main idea of this re-sampling procedure is to eliminate the particles having low weights by re-sampling $\{\mathbf{x}^{\kappa*}_{j,p}, w^{\kappa*}_{j,p}\}^{N}_{p=1}$ from $\{\mathbf{x}^{\kappa}_{j,p}, w^{\kappa}_{j,p}\}^{N}_{p=1}$ with the probability of $p(\mathbf{x}^{\kappa*}_{j,p} = \mathbf{x}^{\kappa}_{j,s}) = w^{\kappa}_{j,s}$. At the end of the resampling procedure, $w^{\kappa*}_{j,p}, p = 1, 2, \ldots, N$ are set as $\frac{1}{N}$. However, the resampling procedure repeats the particles with high weights a number of times stochastically. This leads to diversity loss of particles.

In this paper, a modified particle filter approach with a new sampling method based on supporting intervals of PDFs is proposed. The advantage of the proposed sampling method is that the latest measurement by sensors is taken into account when particles are sampled. Moreover, a mixture Gaussian is used to represent the PDF of the target state instead of a set of properly weighted and located point-mass approximation by Dirac delta function in order to avoid the degeneracy phenomenon.

3.2 Potential Field

The potential field method is a robot motion planning technique that uses an artificial potential function to find the obstacle-free path in an Euclidean workspace. The geometries and positions of the obstacles and targets are considered as sources to construct a potential function U which represents the characteristics of the workspace. Although different approaches have been proposed to generate the potential function based on obstacles' geometries,[32–34] typically the potential function consists of two components, the repulsive potential U_{rep} generated by the obstacles,[35] and the attractive potential U_{att} generated by the robot goal configuration,

$$U(\mathbf{q}) = U_{att}(\mathbf{q}) + U_{rep}(\mathbf{q}) \tag{11}$$

where $\mathbf{q} = [x\ y\ \theta]^T$ is the robot configuration in $\mathcal{W}$, which specifies the robot's position (x and y coordinates) and orientation (θ) with respect to $\mathcal{F}_{\mathcal{W}}$.[35] Recently, an information potential approach was developed for generating an attractive potential based on target geometries and information value in sensor path planning problems, such as the treasure hunt.[36] Once the potential is generated, a virtual force is applied on the robot that is proportional to the negative gradient of U, and can be implemented through a suitable control law, such that U constitutes a Lyapunov function that may be utilized to prove closed-loop stability.

For a robot with a finite platform geometry $\mathcal{A}$, the potential field is generated by taking into consideration the robot configuration space $\mathcal{C}$, and the corresponding obstacles' geometries $\mathcal{B}$. A C-obstacle is defined as the subset of $\mathcal{C}$ that causes collisions with at least one obstacle in $\mathcal{W}$, i.e., $\mathcal{CB}_l \equiv \{\mathbf{q} \in \mathcal{C} \mid \mathcal{A}(\mathbf{q}) \cap \mathcal{B}_l \neq \emptyset\}$, where $\mathcal{A}(\mathbf{q})$ denotes the subset of $\mathcal{W}$ occupied by the platform geometry $\mathcal{A}$ when the robot is at the configuration $\mathbf{q}$. The union of all C-obstacles in $\mathcal{W}$ is referred to as the C-obstacle region. Thus, in searching for targets in $\mathcal{W}$, the robotic sensor is free to rotate and translate in the free configuration space, which is defined as the complement of the C-obstacle region $\mathcal{CB}$ in $\mathcal{C}$, i.e., $\mathcal{C}_{free} = \mathcal{C} \backslash \mathcal{CB}$.[35]

Then, the repulsive potential can be represented as,

$$U_{rep}(\mathbf{q}) = \begin{cases} \frac{1}{2}\eta(\frac{1}{\rho(\mathbf{q})} - \frac{1}{\rho_0})^2 & \text{if} \quad \rho(\mathbf{q}) \leq \rho_0 \\ 0 & \text{if} \quad \rho(\mathbf{q}) > \rho_0 \end{cases} \tag{12}$$

where η is a scaling factor, $\rho(\mathbf{q})$ is the distance between the robot and the nearest obstacle in Euclidean space, and ρ_0 is a constant parameter that is chosen by the user. The attractive potential is given by,

$$U_{att}(\mathbf{q}) = \frac{1}{2}\varepsilon\rho^2_{goal}(\mathbf{q}) \tag{13}$$

where ε is a scaling factor, and $\rho_{goal}(\mathbf{q})$ is the distance between the robot and the goal configuration. In (12) and (13), only the obstacle closest to $\mathbf{q}$ is considered to generate $U_{rep}(\mathbf{q})$, and the target is assumed to be a single point in $\mathcal{C}_{free}$. This makes the potential function difficult to update when new obstacles and targets are sensed during the path execution, because for each value of $\mathbf{q}$, the potential needs to update by computing its distance from the closest obstacle and target.

In this paper, a modified potential function that taking the target Markov properties into account is proposed in order to shorten sensors' traveling distance. Furthermore, when the geometric distance ρ between the sensor platform and nearest target is smaller than ρ_0, the target is treated as an obstacle, while ρ is greater than ρ_1, the target is treated as a target.

4. METHODOLOGY

The methodology presented in this paper obtains a potential-field based control law for an MSA, to surveil a target based on the tracking information provided by a modified particle filter. For simplicity, it is assumed that the target velocity is known and constant, and the time instants at which the discontinuities take place are known and occur at constant intervals. However, the methodology can be generalized, and these assumptions relaxed, by computing the probability density functions (PDFs) of all Markov parameters using the proposed particle filter. Here, the particle filter technique is used to obtain the PDF of the target heading, and to update it with every new measurement $\mathbf{z}_j^\kappa$ over time. In the proposed method, a finite normal mixture is utilized to represent the PDF of the target heading,

$$f(\theta) = \sum_{\ell=1}^{m} \pi_\ell \mathcal{N}(\theta \mid \mu_\ell, \sigma_\ell^2), \quad \sum_{\ell=1}^{m} \pi_\ell = 1, \quad 0 \leq \pi_\ell \tag{14}$$

where $f(\cdot)$ is used to denote a PDF of the arguments in parenthesis, m is the number of normal components, which is assigned a user-defined upper limit M. μ_ℓ and σ_ℓ are the mean and variance for ℓth normal component. Prior to obtaining target measurements, the number of components is set to $m = M$, μ_ℓ is uniformly sampled from the interval $[-\pi \ \pi]$, and σ_ℓ is chosen equal to a user-defined value σ_0. Let $\mathbf{z}_j^\kappa$ denote the measurement obtained by sensor i at t^κ, as shown in (7). Then, the PDF of the jth target's heading at t_κ, based on the set Z_j^κ, modeled by the finite normal mixture,

$$f(\theta_j^\kappa \mid Z_j^\kappa) \leftarrow \sum_{\ell=1}^{m} \pi_{j,\ell}^\kappa \mathcal{N}(\theta_j^\kappa \mid \mu_{j,\ell}^\kappa, (\sigma_{j,\ell}^\kappa)^2) \tag{15}$$

is updated based on the target transition probability function (5). Since the change in the target state is characterized by a Gaussian distribution, i.e.,

$$\theta_j^{\kappa+1} - \theta_j^k \sim \mathcal{N}(\mu, \sigma^2) \tag{16}$$

then, the distribution of $\theta_j^{\kappa+1}$ given Z_j^κ without considering $\mathbf{z}_j^{\kappa+1}$ is given by ,

$$\begin{aligned} \theta_j^{\kappa+1} \mid Z_j^\kappa \quad &\sim \quad \mathcal{N}(\mu, \sigma^2) + \sum_{\ell=1}^{m} \pi_{j,\ell}^\kappa \mathcal{N}(\mu_{j,\ell}^\kappa, (\sigma_{j,\ell}^\kappa)^2) \\ &\sim \quad \sum_{\ell=1}^{m} \pi_{j,\ell}^\kappa (\mathcal{N}(\mu, \sigma^2) + \mathcal{N}(\mu_{j,\ell}^\kappa, (\sigma_{j,\ell}^\kappa)^2)) \\ &\sim \quad \sum_{\ell=1}^{m} \pi_{j,\ell}^\kappa \mathcal{N}(\mu_{j,\ell}^\kappa + \mu, (\sigma_{j,\ell}^\kappa)^2 + \sigma^2) \end{aligned} \tag{17}$$

Thus, the PDF of the target heading at $t_{\kappa+1}$ is given by

$$f(\theta_j^{\kappa+1} \mid Z_j^\kappa) = \sum_{\ell=1}^{m} \pi_{j,\ell}^\kappa \mathcal{N}(\theta_j^{\kappa+1} \mid \mu_{j,\ell}^\kappa + \mu, (\sigma_{j,\ell}^\kappa)^2 + \sigma^2) \tag{18}$$

When the measurement $\mathbf{z}_j^{\kappa+1}$ is considered, Bayes' rule is utilized to obtain $f(\theta_j^{\kappa+1} \mid Z_j^{\kappa+1})$, based on $\mathbf{z}_j^{\kappa+1}$ and $f(\theta_j^{\kappa+1} \mid Z_j^\kappa)$, as follows,

$$\begin{aligned} f(\theta_j^{\kappa+1} \mid Z_j^{\kappa+1}) &\leftarrow f(\theta_j^{\kappa+1} \mid \mathbf{z}_j^{\kappa+1}, Z_j^\kappa) \\ &= \frac{f(\mathbf{z}_j^{\kappa+1} \mid \theta_j^{\kappa+1}, Z_j^\kappa) f(\theta_j^{\kappa+1} \mid Z_j^\kappa)}{f(\mathbf{z}_j^{\kappa+1} \mid Z_j^\kappa)} \\ &\propto f(\mathbf{z}_j^{\kappa+1} \mid \theta_j^{\kappa+1}, Z_j^\kappa) f(\theta_j^{\kappa+1} \mid Z_j^\kappa) \end{aligned} \tag{19}$$

where $f(\mathbf{z}_j^{\kappa+1} \mid \theta_j^{\kappa+1}, Z_j^\kappa)$ can be determined from the measurement model,

$$\begin{aligned} f(\mathbf{z}_j^{\kappa+1} \mid \theta_j^{\kappa+1}, Z_j^\kappa) &\approx f(\mathbf{z}_j^{\kappa+1} \mid \theta_j^{\kappa+1}, \tilde{\mathbf{x}}_j^\kappa) \\ &= \frac{1}{\sqrt{2\pi}\| \sum_j \|} \exp\left(-\frac{\|\mathbf{z}_j^\kappa - \tilde{\mathbf{x}}_j^\kappa - \delta v \begin{bmatrix} \cos(\theta_j^{\kappa+1}) \\ \sin(\theta_j^{\kappa+1}) \end{bmatrix} \|^2}{2\| \sum_j \|^2}\right) \end{aligned}$$

where $\sum_j$ is the covariance, v is the target linear velocity, $\tilde{\mathbf{x}}_j^\kappa$ is the target position estimation obtained at t^κ. To evaluate equation (19), the modified particle filter is used, in which the importance density function is based on the supporting intervals of distributions. $f(\mathbf{z}_j^\kappa \mid \theta_j^{\kappa+1}, Z_j^\kappa)$ and $f(\theta_j^{\kappa+1} \mid Z_j^\kappa)$ are both considered as distributions of $\theta_j^{\kappa+1}$. Let S denote the support interval. Let R denote the definitive range for a distribution. S of $f(x)$ is defined as $f(x) > \gamma, \forall x \in S$. Let S_j^m denote the support interval of $f(\mathbf{z}_j^\kappa \mid \theta_j^{\kappa+1}, Z_j^\kappa)$ and S_j^p denote the support interval of $f(\theta_j^{\kappa+1} \mid Z_j^\kappa)$. Then, $S = S_j^m \cup S_j^p$. The importance density function for sampling particles is defined as

$$f(\theta_j^{\kappa+1}) = \begin{cases} \frac{1}{L} & \text{if } \theta_j^{\kappa+1} \in S \\ 0 & \text{else} \end{cases} \tag{20}$$

where

$$L = \int_R g(\theta_j^{\kappa+1}) d\theta_j^{\kappa+1}, \qquad g(\theta_j^{\kappa+1}) = \begin{cases} 1 & \text{if } \theta_j^{\kappa+1} \in S \\ 0 & \text{else} \end{cases} \tag{21}$$

The weight for each particle is obtained by considering the target state likelihood function and the previous target state estimation together simultaneously. By considering $f(\mathbf{z}_j^{\kappa+1} \mid \theta_j^{\kappa+1}, Z_j^\kappa)$ and $f(\theta_j^{\kappa+1} \mid Z_j^\kappa)$, the weight $w_{j,p}^{\kappa+1}$ for pth particle of jth target, denoted as $\theta_{j,p}^{\kappa+1}$, is set as

$$w_{j,p}^{\kappa+1} = f(\mathbf{z}_{j,p}^{\kappa+1} \mid \theta_{j,p}^{\kappa+1}, Z_j^\kappa) f(\theta_{j,p}^{\kappa+1} \mid Z_j^\kappa) \tag{22}$$

The weight for each particle is normalized via

$$w_{j,p}^{\kappa+1} = \frac{w_{j,p}^{\kappa+1}}{\sum_{p=1}^{N} w_{j,p}^{\kappa+1}} \tag{23}$$

Then weighted EM algorithm, shown in Table 1, is adopted to obtain a normal mixture representation of the target heading's PDF, using weighted particles. After the target heading is obtained, the target position is estimated based on the sensor measurement over the latest time interval, using the least square error method.

In order to maintain the desired distance ρ_{ij} between sensor i and target j within the desired range (1), a new potential function is presented, such that when the distance from the sensor to the target is less than ρ_0,

Table 1. Weighted EM Algorithm

Initialize $\sum_{\ell=1}^{M} \pi_{j,\ell}^{\kappa+1} \mathcal{N}(\mu_{j,\ell}^{\kappa+1}, \sigma_{j,\ell}^{\kappa+1})$ as $\sum_{\ell=1}^{M} \pi_{j,\ell}^{\kappa} \mathcal{N}(\mu_{j,\ell}^{\kappa}, \sigma_{j,\ell}^{\kappa})$
Iterate until $\sum_{\ell=1}^{M} \pi_{j,\ell}^{\kappa+1} \mathcal{N}(\mu_{j,\ell}^{\kappa+1}, \sigma_{j,\ell}^{\kappa+1})$ converges
    for each particle p
        $f_{p,\ell} = \pi_{j,\ell}^{\kappa+1} \mathcal{N}(\theta_{j,p}^{\kappa+1} \mid \mu_{j,\ell}^{\kappa+1}, \sigma_{j,\ell}^{\kappa+1})$
        cluster pth particle into group G_l if $f_{p,\ell} \geq f_{p,r\neq\ell}$
    end
    for each group ℓ
        $\mu_{j,\ell}^{\kappa+1} = \frac{\sum w_{j,p}^{\kappa+1} \theta_{j,p}^{\kappa+1}}{\sum w_{j,p}^{\kappa+1}}, \quad \theta_{j,p}^{\kappa+1} \in G_\ell$
        $\sigma_{j,\ell}^{\kappa+1} = \frac{\sum w_{j,p}^{\kappa+1} (\theta_{j,p}^{\kappa+1} - \mu_{j,\ell}^{\kappa+1})^2}{\sum w_{j,p}}, \quad \theta_{j,p}^{\kappa+1} \in G_\ell$
        $\pi_{j,\ell}^{\kappa+1} = \sum w_{j,p}^{\kappa+1}, \quad \theta_{j,p}^{\kappa+1} \in G_\ell$
    end
    if $\pi_{j,\ell}^{\kappa+1} \leq \zeta$
        set $\pi_{j,\ell}^{\kappa+1} = 0$
    end
end

U becomes a repulsive potential, when the distance is greater than ρ_1, U becomes an attractive potential, and otherwise U is zero. Let $\mathbf{q}_i^\kappa$ denote the configuration of sensor i, and $\mathbf{q}_j^\kappa$ denote the configuration of target j at t_κ. Without considering the knowledge of targets' Markov property, the potential function for the ith sensor at time t_κ would be defined as,

$$U(\mathbf{q}_i^\kappa) = \begin{cases} \frac{1}{2}\eta(\frac{1}{\rho(\mathbf{q}_j^\kappa, \mathbf{q}_i^\kappa)} - \frac{1}{\rho_0})^2, & \text{if } \rho(\mathbf{q}_j^\kappa, \mathbf{q}_i^\kappa) \leq \rho_0 \\ 0, & \text{if } \rho_0 < \rho(\mathbf{q}_j^\kappa, \mathbf{q}_i^\kappa) < \rho_1 \\ \frac{1}{2}\xi(\rho(\mathbf{q}_j^\kappa, \mathbf{q}_i^\kappa) - \rho_1)^2, & \text{if } \rho(\mathbf{q}_j^\kappa, \mathbf{q}_i^\kappa) \geq \rho_1 \end{cases} \tag{24}$$

and this potential field is referred as the exact potential field. In order to shorten sensors' travelling distance, the heading of the target during next segment, denoted as θ^{k+1}, is considered when potential field is constructed. The expectation of θ^{k+1}, denoted by $\tilde{\theta}^{k+1}$, is obtained via equation (5),

$$\tilde{\theta_j}^{k+1} = \mathbb{E}\{\theta_j{}^{k+1}\} = \sum_{\ell=1}^{m} \pi_{j,\ell}^\kappa \theta_{j,\ell}^\kappa + \mu$$

Then the potential field that takes knowledge of target motion into account can be established via

$$U(\mathbf{q}_i^\kappa) = \begin{cases} \frac{1}{2}\eta(\frac{1}{\rho(\mathbf{q}_j^\kappa, \mathbf{q}_i^\kappa)} - \frac{1}{\rho_0})^2, & \text{if } \rho(\mathbf{q}_j^\kappa, \mathbf{q}_i^\kappa) \leq \rho_0 \\ 0, & \text{if } \rho_0 < \rho(\mathbf{q}_j^\kappa, \mathbf{q}_i^\kappa) < \rho_1 \\ \frac{1}{2}\xi(\rho(\mathbf{q}^{\kappa *}, \mathbf{q}_i^\kappa) - \rho_1)^2, & \text{if } \rho(\mathbf{q}_j^\kappa, \mathbf{q}_i^\kappa) \geq \rho_1 \end{cases} \tag{25}$$

where

$$\mathbf{q}^{\kappa *} = \mathbf{q}_j^\kappa + \alpha \begin{bmatrix} \cos\tilde{\theta}_j^{k+1} \\ \sin\tilde{\theta}_j^{k+1} \end{bmatrix} (\rho(\mathbf{q}_j^\kappa, \mathbf{q}_i^\kappa) - \rho_1) \tag{26}$$

where the parameter α is a constant, $\mathbf{q}_j^\kappa$ and $\mathbf{q}_i^\kappa$ are the target and the sensor configurations respectively. This potential field is referred as the virtual potential field, which is different from the one established by equation (24). When the distance between the sensor and the target is in predefined interval, $\mathbf{q}^{\kappa *} = \mathbf{q}_j^\kappa$, which indicates the virtual potential field converges to the exact potential field. The artificial force is provided by the negative gradient of U,

$$\mathbf{F}(\mathbf{q}_i^\kappa) = -\nabla U(\mathbf{q}_i^\kappa), \tag{27}$$

where, from (24), the force provided by the potential field is given by,

$$F(\mathbf{q}_i^\kappa) = \begin{cases} \eta(\frac{1}{\rho(\mathbf{q}_j^\kappa,\mathbf{q}_i^\kappa)} - \frac{1}{\rho_0})\frac{\nabla\rho(\mathbf{q}^{\kappa*},\mathbf{q}_i^\kappa)}{\rho^2(\mathbf{q}^{\kappa*},\mathbf{q}_i^\kappa)} & \text{if } \rho(\mathbf{q}_j^\kappa,\mathbf{q}_i^\kappa) \le \rho_0 \\ 0 & \text{if } \rho_0 < \rho(\mathbf{q}_j^\kappa,\mathbf{q}_i^\kappa) < \rho_1. \\ -\xi(\rho(\mathbf{q}^{\kappa*},\mathbf{q}_i^\kappa) - \rho_1)\nabla\rho(\mathbf{q}^{\kappa*},\mathbf{q}_i^\kappa) & \text{if } \rho(\mathbf{q}_j^\kappa,\mathbf{q}_i^\kappa) \ge \rho_1 \end{cases} \tag{28}$$

Then, similar to,[37,38] the control law $\mathbf{u}$ defined in terms of the artificial force is,

$$\mathbf{u}(\mathbf{q}_i^\kappa) = (\dot{\mathbf{x}}_j^\kappa - \mathbf{v}_i^\kappa) + F(\mathbf{q}_i^\kappa). \tag{29}$$

The Lyapunov function

$$V = \frac{1}{2}(\dot{\mathbf{x}}_j^\kappa - \mathbf{v}_i^\kappa)^T(\dot{\mathbf{x}}_j^\kappa - \mathbf{v}_i^\kappa) + U(\mathbf{q}_i^\kappa) \tag{30}$$

is considered as a possible positive semidefinite candidate, in order to analyze the stability of the control law (29). From (2), (29), and (30), the time derivative of the chosen Lyapunov function is given by:

$$\begin{aligned} \dot{V} &= (\dot{\mathbf{x}}_j^\kappa - \mathbf{v}_i^\kappa)(-\dot{\mathbf{v}}_i^\kappa) - \nabla U(\mathbf{q}_i^\kappa)(\dot{\mathbf{x}}_j^\kappa - \mathbf{v}_i^\kappa) \\ &= (\dot{\mathbf{x}}_j^\kappa - \mathbf{v}_i^\kappa)(-(\dot{\mathbf{x}}_j^\kappa - \mathbf{v}_i^\kappa) + \nabla U(\mathbf{q}_i^\kappa)) - \nabla U(\mathbf{q}_i^\kappa)(\dot{\mathbf{x}}_j^\kappa - \mathbf{v}_i^\kappa) \\ &= -(\dot{\mathbf{x}}_j^\kappa - \mathbf{v}_i^\kappa)^T(\dot{\mathbf{x}}_j^\kappa - \mathbf{v}_i^\kappa) \le 0 \end{aligned} \tag{31}$$

Furthermore, $V \ge 0$ because $U(\mathbf{q}_i^\kappa) \ge 0$. Thus, considering $\dot{V} \le 0$, the system under the control law (29) is asymptotically stable.

5. SIMULATIONS AND RESULTS

To determine the effectiveness of the proposed methodologies, simulations are run in two different scenarios. The first, which is primarily used to test the modified particle filter, does not consider the geometries of the sensor and target, as they are modeled as point masses. The second scenario addresses the geometries of both sensor and target, and includes obstacles in the workspace. Scenario 1, as previously stated, models the sensor platform and the target as point masses. The workspace is defined as an obstacle free area with dimensions 50m × 50m. A single target, that changes its heading every 10 s, maneuvers the environment at a speed of 2m/s. The sensor, with an omnidirectional FOV of radius 10m, is deployed in order to track the target. The position of the target is measured every 0.3 s by the sensor, and it is assumed that the measurements have a standard deviation, Σ = diag(0.4, 0.4). To determine the effectiveness of the modified particle filter, the estimation error of the target heading inference is calculated. The estimation error, for a time interval, is defined as

$$\epsilon = \tilde{\theta^\kappa} - \theta^\kappa \tag{32}$$

where $\tilde{\theta^\kappa}$ is the target heading estimation, and θ^κ is the true value of the target heading.

The estimation error associated with the modified particle filter in the first scenario is shown Fig. 1. As seen in the plot, at the beginning of the simulation, the initial estimation of the heading varies greatly with the targets actual heading, but converges to it quickly. The spikes denoted by $k = 1$ and $k = 2$ in the plot correspond to a change in the targets heading direction, as explained above. The estimation error grows dramatically when the target suddenly changes its direction. As the sensor updates its measurements, the estimation error, once again, quickly converges to zero. The simulations for the first scenario, although simple, exhibit the effectiveness of the modified particle filter in estimating the heading position of the target, and therefore the tracking abilities of the sensor.

The simulations of the second scenario, which consider finite target and platform geometries, also implement the dynamics used in scenario 1. However, the workspace is expanded to 100m × 10m, and is populated with seven obstacles, modeled as convex polygons. For these simulations, the objective of the sensor is to maintain the distance ρ_{ij}, from the sensor to the target, between 3m and 4m, while avoiding the obstacles. The results of the simulations for scenario 2 can be found in Fig. 2, and Fig. 3 shows the path of the sensor platform, $\mathcal{A}$,

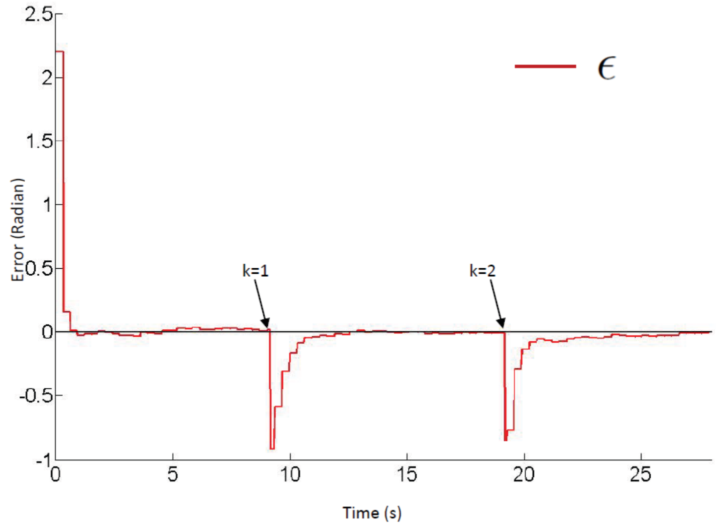

Figure 1. Target heading estimation

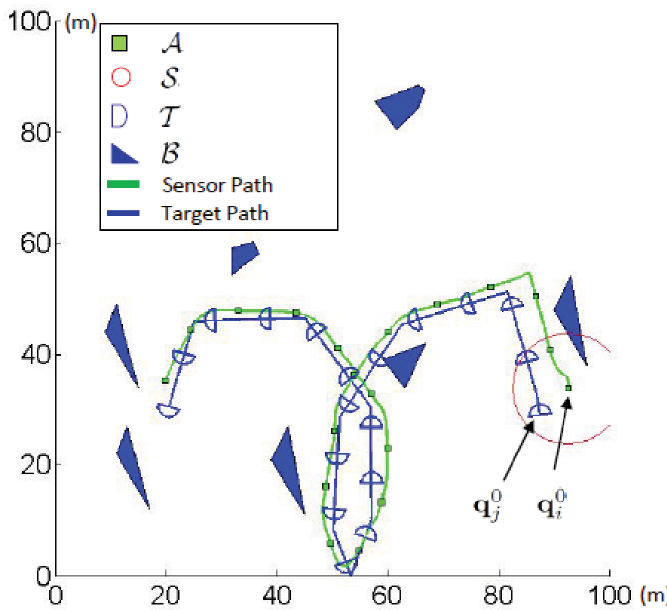

Figure 2. Path example

with FOV $\mathcal{S}$, as it tracks the movement of the target, denoted as $\mathcal{T}$. Moreover, $\mathbf{q}_j^0$ and $\mathbf{q}_i^0$ indicate the initial positions of the target and the sensor separately. The Euclidean distance between the sensor and the target along the path is in Fig. 3, where the vertical dashed lines indicate the instants t_k, with $k = 1, 2, \ldots$, when the target changes its heading. Figure. 3 shows large changes in the geometric distance between the sensor platform and the target, ρ_{ij}, when the target changes its heading. However, ρ_{ij} quickly converges back to the required

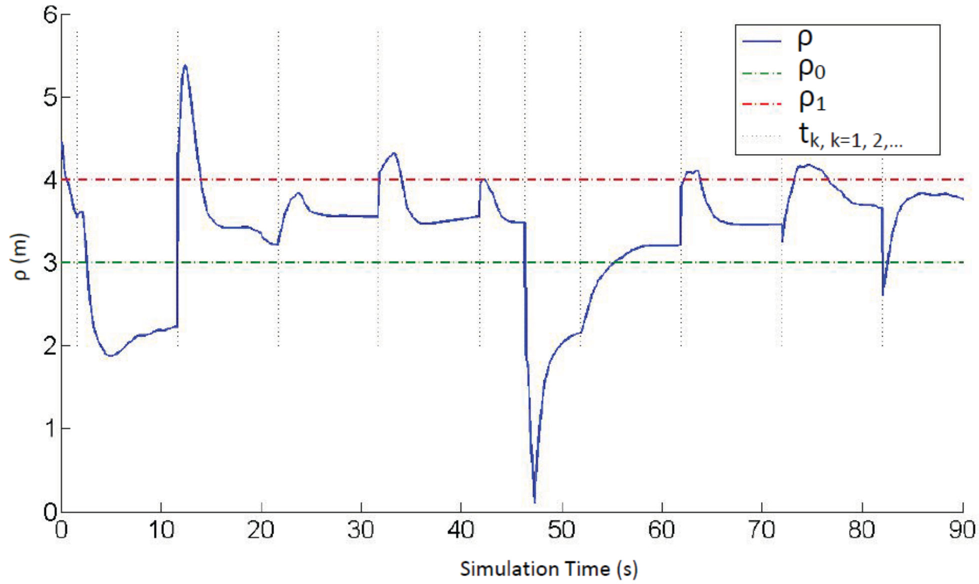

Figure 3. Geometric distance between sensor i and target j.

range, $\rho_0 \leq \rho_{ij} \leq \rho_1$, where $\rho_0 = 3$m, and $\rho_1 = 4$m. The simulations demonstrate that the potential field method presented in this paper is capable of maintaining the sensor within a desired distance from the target. Furthermore, the proposed sampling method, as seen in this analysis, supports the claim that the noise of the sensor measurements can be non-Gaussian.

6. CONCLUSIONS AND FUTURE WORK

This paper presents an information potential approach for computing the MSAs' motion plans and control inputs based on the feedback from a modified particle filter used for tracking moving targets. The modified particle filter, as presented in this paper implements a new sampling method (based on supporting intervals of density functions), which accounts for the latest sensor measurements and adapts, accordingly, a mixture representation of the probability density functions (PDFs) for the target motion. The proposed methodology is such that the importance density of the particles is a function of the current measurement distribution and the distribution of the previous estimation. Furthermore, a modified potential field method, which considers the Markov property of a target, is proposed in order to decrease the traveling distance of a sensor, as compared to the traditional potential field method. The heading of a target is estimated by the particle filter using the proposed supporting interval sampling method and mixture Gaussian representation of the target state estimation. In future work, this method will be extended to the multivariable case, in which not just the targets' heading and positions, are estimated online from the sensor measurements. The methodology will also be implemented for sensors that have directional FOVs, with noise that is non-Gaussian.

Acknowledgment

This work is supported by NSF grant ECCS #1028506.

REFERENCES

1. S. Ferrari, C. Cai, R. Fierro, and B. Perteet, "A multi-objective optimization approach to detecting and tracking dynamic targets in pursuit-evasion games," in *Proc. of the 2007 American Control Conference*, pp. 5316–5321, (New York, NY), 2007.
2. D. Culler, D. Estrin, and M. Srivastava, "Overview of sensor networks," *Computer* **37**(8), pp. 41–49, 2004.
3. P. Juang, H. Oki, Y. Wang, M. Martonosi, L. Peh, and D. Rubenstein, "Energy efficient computing for wildlife tracking: Design tradeoffs and early experiences with zebranet," *Proc. 10^{t}h International Conference on Architectural Support for Programming Languages and Operating Systems (ASPLOS-X)* , 2002.
4. C. Cai and S. Ferrari, "Information-driven sensor path planning by approximate cell decomposition," *IEEE Transactions on Systems, Man, and Cybernetics - Part B* **39**(3), pp. 607–625, 2009.
5. P. Cheng, G. Pappas, and V. Kumar, "Decidability of motion planning with differential contraints," in *Proceedings of the 46nd IEEE International Conference on Robotics and Automation*, pp. 1826–1831, (Roma Italy), 2007.
6. S. Ferrari, R. Fierro, B. Perteet, C. Cai, and K. Baumgartner, "A geometric optimization approach to detecting and intercepting dynamic targets using a mobile sensor network," *SIAM Journal on Control and Optimization* **48**(1), pp. 292–320, 2009.
7. K. Baumgartner and S. Ferrari, "A geometric transversal approach to anayzing track coverage in sensor networks," *IEEE Transactions on Computers* **57**(8), 2008.
8. G. Zhang, S. Ferrari, and M. Qian, "Information roadmap method for robotic sensor path planning," *Journal of Intelligent and Robotic Systems* **56**(1-2), pp. 69–98, 2009.
9. S. Ferrari and C. Cai, "Information-driven search strategies in the board game of clue," *IEEE Transactions on Systems, Man, and Cybernetics - Part B* **39**(3), pp. 607–625, 2009.
10. V. Isler, C. Belta, K. Daniilidis, and G. Pappas, "Hybrid control for visibility-based pursuit-evasion games," in *Proc. of 2004 IEEE/RSJ International Conference on Intelligent Robots and Systems*, pp. 1432–1437, (Sendai, Japan), 2004.
11. L. Lulu and A. Elnagar, "A comparative study between visibility-based roadmap path planning algorithms," in *IEEE/RSJ International Conference on Intelligent Robots and Systems*, pp. 3263 – 3268, 2005.
12. S. Bhattacharya, R. Murrieta-Cid, and S. Hutchinson, "Optimal paths for landmark-based navigation by differential-drive vehicles with field-of-view constraints," *Robotics, IEEE Transactions on* **23**(1), pp. 47 –59, 2007.
13. M. Baumann, S. Leonard, E. Croft, and J. Little, "Path planning for improved visibility using a probabilistic road map," *Robotics, IEEE Transactions on* **26**(1), pp. 195 –200, 2010.
14. Y. BarShalom, X. R. Li, and T. Kirubarajan, *Estimation with Applications to Tracking and Navigation: Algorithms and Software for Information Extraction*, Wiley and Sons, 2001.
15. Y. BarShalom and W. D. Blair, *MultitargetMultisensor Tracking: Applications and Advances*, Artech House, 2000.
16. Y. BarShalom and X. R. Li, *MultitargetMultisensor Tracking: Principles and Techniques*, YBS Publishing, 1995.
17. S. S. Blackman, *Multiple-Target Tracking with Radar Applications*, Artech House, 1986.
18. C. L. Morefiled, "Decision-directed approach to multitarget tracking," *IEEE Trans. on Automatic Control* **22**(3), 1977.
19. G. B. G. Welch, "An introduction to the kalman filter," tech. rep., Department of Computer Science, University of North Carolina at Chapel Hill.

20. S. J. Julier and J. K. Uhlmann, "A new extension of the kalman filter to nonlinear systems," *Proc. AeroSense: 11th Int. Symp. Aerospace/Defense Sensing, Simulation and Controls, pp. 182-197* , 1997.
21. E. Wan and R. Van Der Merwe, "The unscented kalman filter for nonlinear estimation," in *Proceedings of the IEEE 2000 Adaptive Systems for Signal Processing, Communications, and Control Symposium*, pp. 153 –158, 2000.
22. S. Julier, "The scaled unscented transformation," in *American Control Conference, 2002. Proceedings of the 2002*, **6**, pp. 4555–4559, 2002.
23. Z. Khan, T. Balch, and F. Dellaert, "An mcmc-based particle filter for tracking multiple interacting targets," in *Computer Vision - ECCV 2004*, T. Pajdla and J. Matas, eds., pp. 279–290, 2004.
24. C. Kreucher, K. Kastella, and O. Hero, "Multitarget tracking using the joint multitarget probability density," *IEEE Transactions on Aerospace and Electronic Systems* **41**(4), pp. 1396–1414, 2005.
25. M. Arulampalam, S. Maskell, N. Gordon, and T. Clapp, "A tutorial on particle filters for online nonlinear/non-gaussian bayesian tracking," *Signal Processing, IEEE Transactions on* **50**(2), pp. 174 –188, 2002.
26. J. Carpenter, P. Clifford, and P. Fearnhead, "Improved particle filter for nonlinear problems," in *Radar, Sonar and Navigation, IEEE Proceedings*, **146**(1), pp. 2 –7, 1999.
27. Y. Rui and Y. Chen, "Better proposal distributions: Object tracking using unscented particle filter," *Computer Vision and Pattern Recognition, IEEE Computer Society Conference on* **2**, 2001.
28. T. W. O'Gorman, *Applied adaptive statistical method: test of sigficance and condifence intervals*, Society for Industrial and Applied Mathematics,Philadelphia, 2004.
29. H. Leung, Z. Hu, and M. Blanchette, "Evaluation of multiple radar target trackers in stressful environments," *IEEE Transactions on Aerospace and Electronic Systems* **35**(2), p. 663 674, 1999.
30. I. J. Cox and M. L. Miller, "On finding ranked assignments with application to multitarget tracking and motion correspondence," *IEEE Transactions on Aerospace and Electronic Systems* **31**, pp. 486–489, 1999.
31. G. o. N Limnios, *Semi-Markov Process and Reliability*, Birkhauser, Boston, 2001.
32. J. Ren and K. Mclsaac, "A hybird-systems approach to potential field navigation for a multi-robot team," in *Proc. of IEEE International Conference on Robotics and Automation*, pp. 3875–3880, (Taipei, Taiwan), 2003.
33. S. Shimoda, Y. Kuroda, and K. Iagnemma, "Potential field navigation of high speed unmanned ground vehicles on uneven terrain," in *Proc. of IEEE International Conference on Robotics and Automation*, pp. 2839–2844, 2005.
34. S. Ge and Y. Cui, "New potential functions for mobile robot path planning," *IEEE Transactions on Robotics and Automation* **16**(5), 2000.
35. J. C. Latombe, *Robot Motion Planning*, Kluwer Academic Publishers, 1991.
36. G.Zhang and S.Ferrari, "An adaptive artificial potential function approach for geometric sensing," in *Proc. of IEEE International Conference on Decision and Control*, pp. 7903–7910, 2009.
37. Z. Yang, Q. Zhang, and Z. Chen, "Flocking of multi-agents with nonlinear inner-coupling function," *Nonlinear Dynamics* **60**(3), pp. 255–264, 2009.
38. S. S. Ge and Y. J. Cui, "Dynamic motion planning for mobile robots using potential field method," *Auton. Robots* **13**(3), pp. 207–222, 2002.